

Crystallization and Morphology of Cholesterol End-Capped Poly(ethylene glycol)

Yuan-Jin Qiu,¹ Jun-Ting Xu,¹ Liang Xue,¹ Zhi-Qiang Fan,¹ Zhong-Hua Wu²

¹Key Laboratory of Macromolecular Synthesis and Functionalization, Department of Polymer Science and Engineering, Zhejiang University, Hangzhou 310027, China

²Beijing Synchrotron Radiation Laboratory, Institute of High Energy Physics, Chinese Academy of Sciences, Beijing 100039, China

Received 24 July 2005; accepted 8 July 2006

DOI 10.1002/app.25362

Published online in Wiley InterScience (www.interscience.wiley.com).

ABSTRACT: Crystallization and morphology of polyethylene glycol with molecular weight $M_n = 2000$ (PEG2000) capped with cholesterol at one end (CS-PEG2000) and at both ends (CS-PEG2000-CS) were investigated. It is found that the bulky cholesteryl end group can retard crystallization rate and decrease crystallinity of PEG, especially for CS-PEG2000-CS. Isothermal crystallization kinetics shows that the Avrami exponent of CS-PEG2000 decreases as crystallization temperature (T_c). The Avrami exponent of CS-PEG2000-CS increases slightly with T_c , but it is lower than that of CS-PEG2000. Compared to the perfect spherulite morphology of PEG2000, CS-PEG2000 exhibits irregular and leaf-like spherulite morphology, while only needle-like crystals are observed in CS-PEG2000-CS. The linear

growth rate of CS-PEG2000 shows a stronger dependence on T_c than PEG2000. The cholesterol end group alters not only the free energy of the folding surface, but also the temperature range of crystallization regime. The small angle X-ray scattering (SAXS) results show that lamellar structures are formed in all these three samples. By comparing the long periods obtained from SAXS with the theoretically calculated values, we find that the PEG chains are extended in PEG2000 and CS-PEG2000, but they are once-folded in CS-PEG2000-CS. © 2006 Wiley Periodicals, Inc. *J Appl Polym Sci* 103: 2464–2471, 2007

Key words: crystallization; poly(ethylene glycol); end group; cholesterol

INTRODUCTION

End groups sometimes play an important role in polymer properties, such as thermal stability,^{1–4} reactivity,^{5–7} aggregation behavior in solution,⁸ and crystallization behavior.⁹ The influence of end groups becomes more important in polymers of low molecular weight due to high proportion of end group.¹⁰ For crystalline polymers, end groups can be viewed as defects and may affect crystallization behavior and morphology of polymers. Cheng et al. reported that end groups drive the change of PEO chains from nonintegrated folding to integrated folding, but larger end groups make such a change proceed very slowly due to friction among end groups.¹¹ So far most of the end groups in PEG are small molecules. Recently, PEGs capped with fullerene or cholesterol,^{12–15} which are relatively more bulky than the small end groups previously used, were prepared. However, crystallization behavior of PEG with large

end group is rarely reported. In this study, PEGs capped with cholesterol at one end and at both ends were synthesized and crystallization behavior and morphology of them were studied.

EXPERIMENTAL

Materials

Cholesterol (ACROS) was purified by recrystallization from ethanol. Polyethylene glycol (PEG) with molecular weight $M_n = 2000$ and $M_w/M_n = 1.06$ (ACROS) and polyethylene glycol ($M_n = 2000$, $M_w/M_n = 1.07$) monomethyl ether (Aldrich) were purified by distillation in toluene just before use to remove absorbed water.

Synthesis of CS-PEG2000

4.0 g PEG monomethyl ether was dissolved in 60 mL chloroform, and 4.03 g terephthaloyl chloride (TPC) was dissolved in 30 mL dry chloroform. The PEG/chloroform solution was slowly dropped into TPC/chloroform solution. The resulting solution was stirred under nitrogen at 65°C for 24 h. Chloroform was removed under vacuum and the excessive TPC in the solid was washed by abundant diethyl ether

Correspondence to: J.-T. Xu (xujt@zju.edu.cn).

Contract grant sponsor: National Natural Science Foundation of China; contract grant number: 20374046.

Contract grant sponsor: Ministry of Education, China.

for at least five times under nitrogen. The residue was dried by vacuum and dissolved in 60 mL chloroform called as solution A. 5 g cholesterol was dissolved in 20 mL chloroform. Solution A was then dropped into cholesterol/chloroform solution slowly, stirred under nitrogen at 65°C for 24 h. The solution was cooled to room temperature and washed by diethyl ether and white solid was precipitated. The solid was dried in vacuum at room temperature for 24 h. The product was characterized with $^1\text{H-NMR}$ on a Bruker AMX500 NMR spectrometer (Rheinstetten, Germany) using deuterated chloroform as solvent [Fig. 1(a)]. The molecular weight distribution (M_w/M_n) of CS-PEG2000 measured by gel-permeation chromatograph (GPC) was 1.06, similar to the raw material.

Synthesis of CS-PEG2000-CS

4.0 g PEG was dissolved in 60 mL chloroform and 8.0 g TPC was dissolved in 40 mL dry chloroform. The PEG/chloroform solution was slowly dropped

into TCL/chloroform solution. The resulting solution was stirred under nitrogen at 65°C for 24 h. Chloroform was removed under vacuum and the excessive TPC in the solid was washed by abundant diethyl ether for at least five times under nitrogen. The residue was dried in vacuum and then dissolved in 60 mL chloroform called as solution B. 10 g cholesterol was dissolved in 30 mL chloroform. Solution B was dropped into cholesterol/chloroform solution slowly, stirred under nitrogen at 65°C for 24 h. The solution was cooled to room temperature and washed by diethyl ether. White solid was precipitated and dried in vacuum at room temperature for 24 h. The product was characterized with $^1\text{H-NMR}$ [Fig. 1(b)]. The molecular weight distribution (M_w/M_n) of CS-PEG2000-CS was 1.08.

Differential scanning calorimetry

Differential scanning calorimetry (DSC) experiments were carried out on a TA Q100 instrument (New Castle, DE). In nonisothermal crystallization, the samples were first held at 80°C for 5 min to erase thermal history, then were cooled to -50°C at a rate of 10°C/min and again heated to 80°C at a rate of 10°C/min. Both cooling and heating DSC traces were recorded. In isothermal crystallization experiments, the samples were held at 80°C for 5 min and then cooled to the desired crystallization temperature at a rate of 100°C/min. The samples were held at crystallization temperature until crystallization was completed. The change of heat flow with time was recorded upon crystallization.

Polarized optical microscopy

An Olympus BX-5 polarized optical microscope (POM) (Tokyo, Japan) equipped with a hot-stage, and a digital camera was used to study morphology of the cholesterol capped PEG under isothermal crystallization conditions. The samples were first melted at 80°C on the hot-stage, and then transferred to another hot-stage at the preset crystallization temperature, T_c , and allowed to crystallize isothermally. The hot-stage was calibrated with standard, sharp-melting substances. During crystallization, the growth of the spherulites was monitored as a function of time and the linear growth rate of spherulites (G) can be determined from the slope in the plot of spherulite radius versus time.

Small angle X-ray scattering

Synchrotron small angle X-ray scattering (SAXS) measurements were performed at beamline 4B9A at Beijing Synchrotron Radiation Facility,¹⁶ using a SAXS apparatus constructed at the station over q

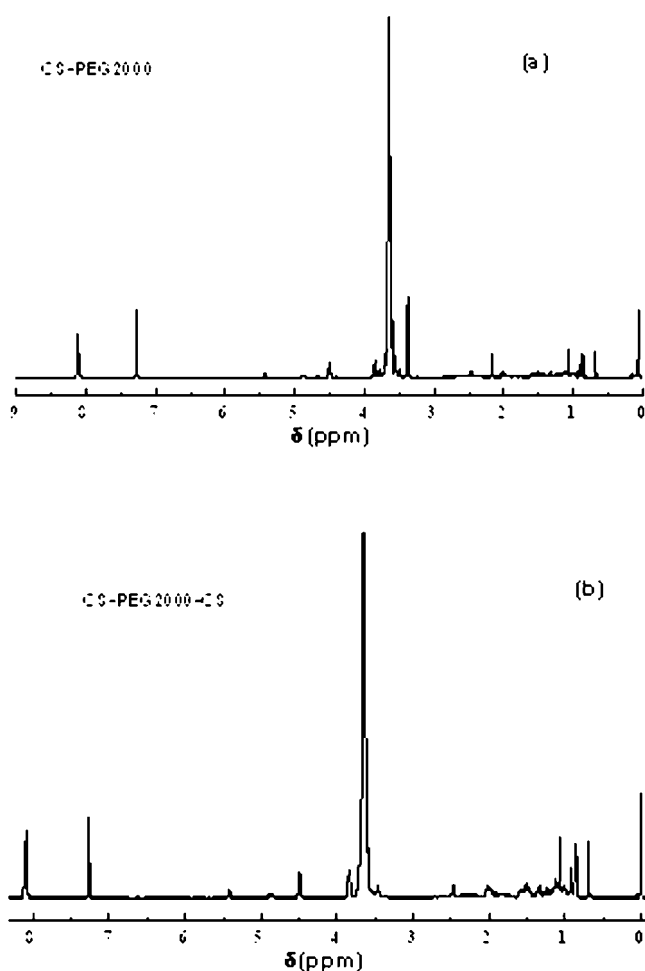


Figure 1 $^1\text{H-NMR}$ spectra of (a) CS-PEG2000 and (b) CS-PEG2000-CS.

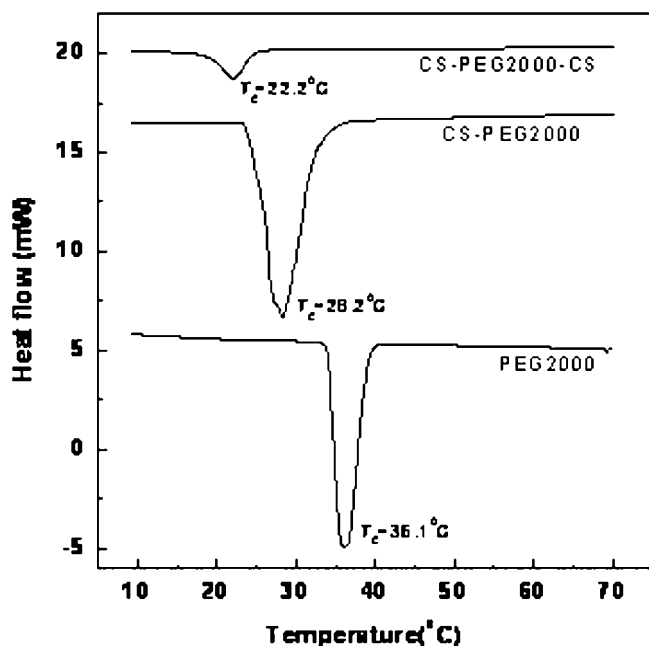


Figure 2 Nonisothermal crystallization DSC traces of PEG2000, CS-PEG2000, and CS-PEG2000-CS.

ranges of $0.005 \text{ \AA}^{-1} < q < 0.15 \text{ \AA}^{-1}$, where $q = 4\pi \sin(\theta/2)/\lambda$, with θ and λ being respectively, the scattering angle and incident X-ray wavelength of 1.54 \AA . The data accumulation time was about 5 min for each sample, depending on the intensity of incident X-ray. The distance between the sample chamber and detector was 1.52 m. The images for scattering of the samples were obtained by an image plate (Mar345) detector. The data were analyzed with a Fit2D program. The samples for SAXS experiments were first heated to melt and cooled to room temperature, and then were annealed 2°C below the melting temperature (determined by DSC) for 12 h.

RESULTS AND DISCUSSION

Nonisothermal crystallization and melting behaviors

Figures 2 and 3 show the nonisothermal crystallization and melting DSC traces of PEG2000, CS-PEG2000, and CS-PEG2000-CS, respectively. It is found that CS-PEG2000 exhibits lower crystallization temperature than uncapped PEG2000, showing that larger supercooling is required for crystallization CS-PEG2000. The crystallization peak of CS-PEG2000 is also broader than that of PEG2000, which means the crystallization rate of PEG is retarded by large cholesterol end-group. For CS-PEG2000-CS, which is capped with cholesterol at both ends, the crystallization temperature shifts further to lower temperature. We notice that the crystallization enthalpy of CS-PEG2000-CS is evidently smaller than that of

PEG2000 and CS-PEG2000, indicating that crystallinity is greatly reduced by the bulky cholesteryl at both ends. No liquid crystalline phase was detected in CS-PEG2000 and CS-PEG2000-CS. This is possibly due to the long PEG chain. In contrast, liquid crystalline phase is retained in cholesterol attached with short PEG chains.¹⁷ One can see from Figure 3 that CS-PEG2000 has similar melting temperature with PEG2000, but CS-PEG2000-CS has much lower melting temperature. This finding will be discussed in terms of SAXS results in the next section.

Isothermal crystallization kinetics

The isothermal crystallization kinetics of polymer can be analyzed using Avrami equation:

$$1 - X(t) = \frac{\Delta H_{t=\infty}^c - \Delta H_t^c}{\Delta H_{t=\infty}^c - \Delta H_{t=0}^c} = \exp(-Kt^n) \quad (1)$$

where $X(t)$ is the relative crystallinity at time t , $\Delta H_{t=\infty}^c$ and ΔH_t^c are the crystallization enthalpies on complete crystallization and after time t . Therefore, we have:

$$\ln[-\ln(1 - X(t))] = \ln K + n \ln t \quad (2)$$

The crystallization rate constant K and Avrami exponent n can be determined from the intercept and slope in the plot of $\ln[-\ln(1 - X(t))]$ versus $\ln(t)$, respectively.

The Avrami plots of CS-PEG2000 and CS-PEG2000-CS at various crystallization temperatures are illus-

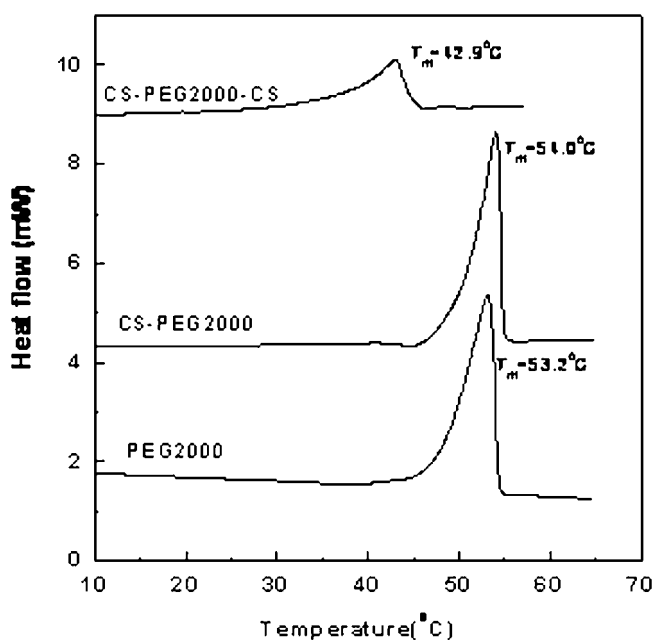


Figure 3 Melting DSC traces of PEG2000, CS-PEG2000, and CS-PEG2000-CS.

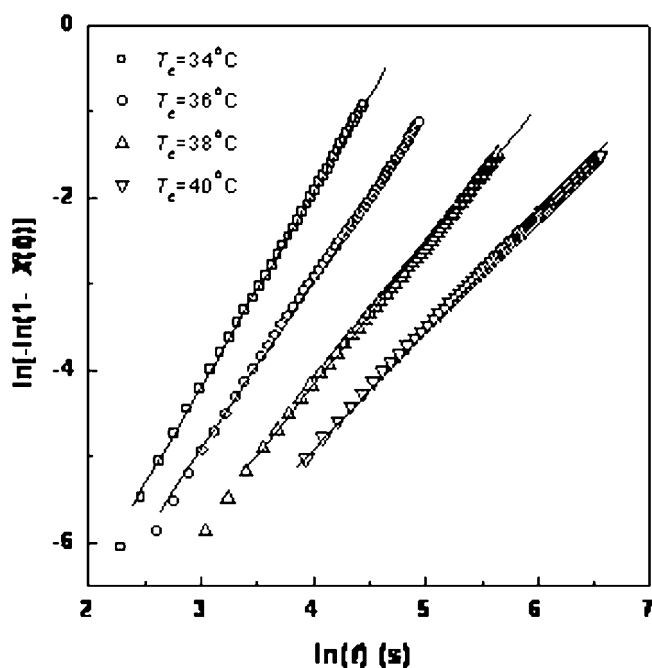


Figure 4 Avrami plots of CS-PEG2000 at various crystallization temperatures.

trated in Figures 4 and 5, respectively, and the obtained values of Avrami exponent and crystallization rate constant are summarized in Table I. The Avrami exponents of CS-PEG2000 at $T_c = 34^\circ\text{C}$ and $T_c = 36^\circ\text{C}$ are around 2.0, which are similar to the values of PEO homopolymer.^{18,19} However, it is found that the Avrami exponents of CS-PEG2000 strongly depend

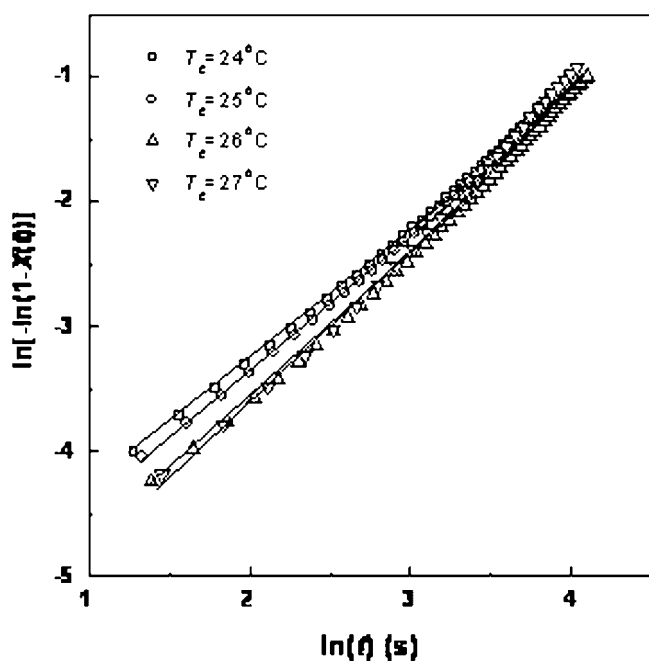


Figure 5 Avrami plots of CS-PEG2000-CS at various crystallization temperatures.

TABLE I
Avrami Exponents and Crystallization Rate Constants of CS-PEG2000 and CS-PEG2000-CS

	T_c ($^\circ\text{C}$)	n	$\ln K$ (s^{-1})
CS-PEG2000	34	2.3	-11.0
	36	1.9	-10.7
	38	1.6	-10.6
	40	1.3	-10.0
CS-PEG2000-CS	24	1	-5.4
	25	1.1	-5.7
	26	1.2	-6.1
	27	1.3	-6.3

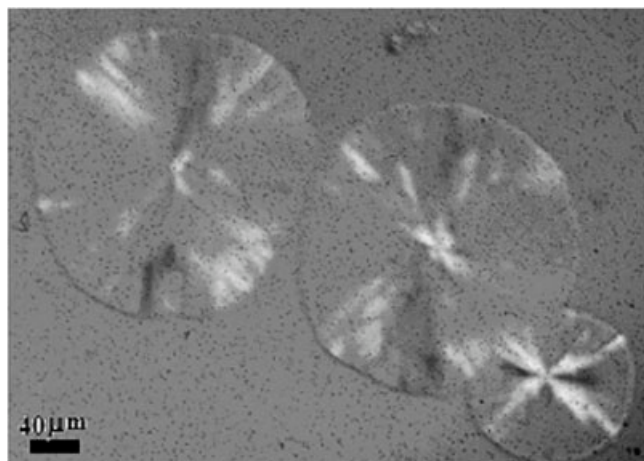
on crystallization temperature. With increase in T_c , the Avrami exponent decreases gradually from 2.3 at $T_c = 34^\circ\text{C}$ to 1.3 at $T_c = 40^\circ\text{C}$. The Avrami exponent is related to growth dimension of polymer crystals. At higher T_c , the polymer crystals generally grow more perfectly and have larger Avrami exponent. As a result, such a phenomenon that Avrami exponent decrease with T_c is quite unusual. The Avrami exponents of CS-PEG2000-CS are around 1.0 and are lower than those of CS-PEG2000. Usually an Avrami exponent $n = 1.0$ is observed for crystallization in a confined environment.²⁰ However, we did not observe a microphase separated structure in the melt of CS-PEG2000-CS by SAXS and liquid crystalline phase was not detected by DSC either, so PEG2000 does not crystallize from a preordered structure, which provide for a confined environment. We speculate that the small Avrami exponent of CS-PEG2000-PEG is the result of the strongly reduced growth dimension of PEG crystals due to the presence of cholesterol end-groups, as can be seen from the superstructure in the next section. It also noticed that the Avrami exponent of CS-PEG2000-CS increases slightly with increase of T_c and exhibits a weaker dependence on T_c . The crystallization rate constants for both CS-PEG2000 and CS-PEG2000-CS do not change much with T_c .

Morphology and linear growth rate of spherulites

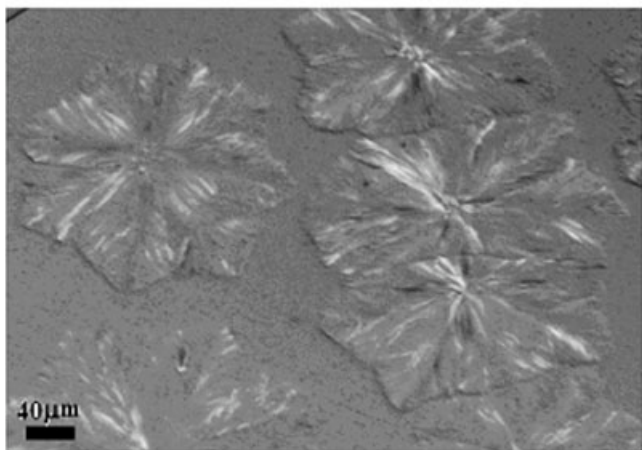
Figure 6 shows the polarized optical micrographs of PEG2000, CS-PEG2000, and CS-PEG2000-2000 during isothermal crystallization. It is observed that PEG2000 exhibits typical spherulite morphology with Maltese crosses. Spherulites with Maltese crosses are observed for CS-PEG2000 as well, but the spherulites are irregular and leaf-like, showing that the PEG crystals grow preferentially in some directions due to the presence of cholesterol end group. In contrast, no spherulites and only needle-like crystals are observed in CS-PEG2000-CS.

The linear growth rates of spherulites (G) for PEG2000 and CS-PEG2000 are illustrated in Figure 7. Since the crystals of CS-PEG2000 are polygonal, the radius is determined in terms of the average values

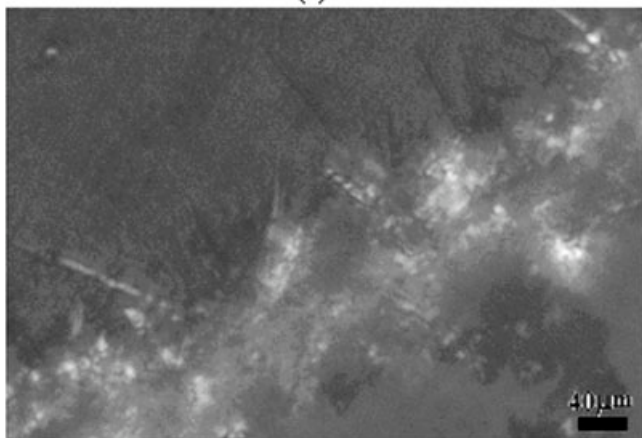
of distances from the center to various corners. It is found that linear growth rates of spherulites decreases as crystallization temperature increase for



(a)



(b)



(c)

Figure 6 Polarized optical micrographs of (a) PEG2000, (b) CS-PEG2000, and (c) CS-PEG2000-CS during isothermal crystallization. The crystallization temperatures are 45°C for PEG2000, 44°C for CS-PEG2000, and 30°C for CS-PEG2000-CS.

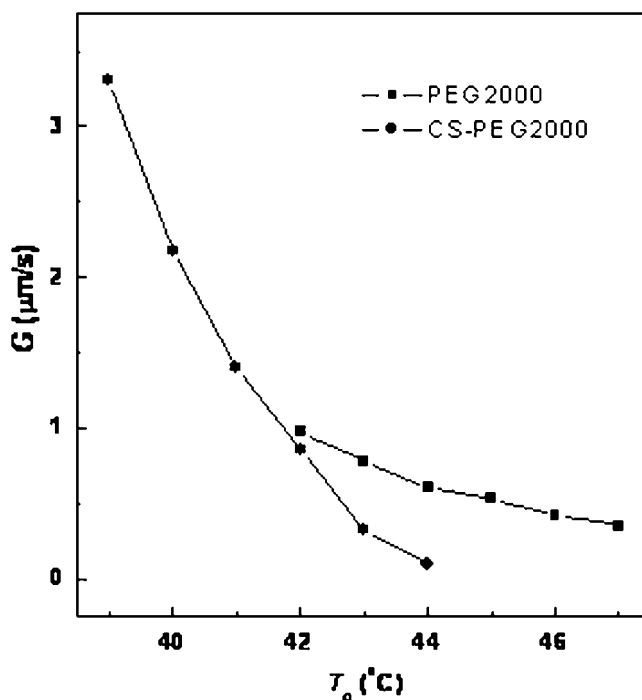


Figure 7 Linear growth rates of spherulites for PEG2000 and CS-PEG2000.

both samples, but obviously CS-PEG2000 exhibits a stronger dependence on crystallization temperature.

Based on the crystallization regime theory of Lauritzen and Hoffman, the linear growth rate (G) of polymer spherulites can be expressed as follows²¹:

$$G = G_0 \exp[-U^*/R(T_c - T_0)] \exp[-K_g/T_c(T_m^0 - T_c)f] \quad (3)$$

where G_0 is a constant and is independent of temperature, U^* is the activation energy related with the short distance diffusion of the crystalline unit across the phase boundary, T_c is crystallization temperature, T_0 is the temperature below which there is no chain motion (usually $T_0 = T_g - 30$ K), f is the correction factor and is equal to $2T_c/(\Delta T_m^0 + T_c)$.

The nucleation constant, K_g , is expressed as:

$$K_g = j b_0 \sigma \sigma_e T_m^0 / k (\Delta h)_f \quad (4)$$

where $j = 4$ for crystallization regimes I and III, and $j = 2$ for crystallization regime II, b_0 is the layer thickness, σ is the lateral surface free energy, σ_e is the free energy of the folding surface, Δh_f is fusion enthalpy, and k is Boltzmann's constant. The values of U^* , ΔT_m^0 , T_g , T_0 , Δh_f , b_0 , and σ are 6.28 kJ/mol, 339.4 K, 206 K, 176 K, 2.30×10^8 J/m³, 4.6 Å, and 10.0 erg/cm²,²² respectively.

Figure 8 shows the plot of $\ln G + U^*/R(T_c - T_0)$ versus $1/T_c(\Delta T)f$ for PEG2000 and CS-PEG2000. A

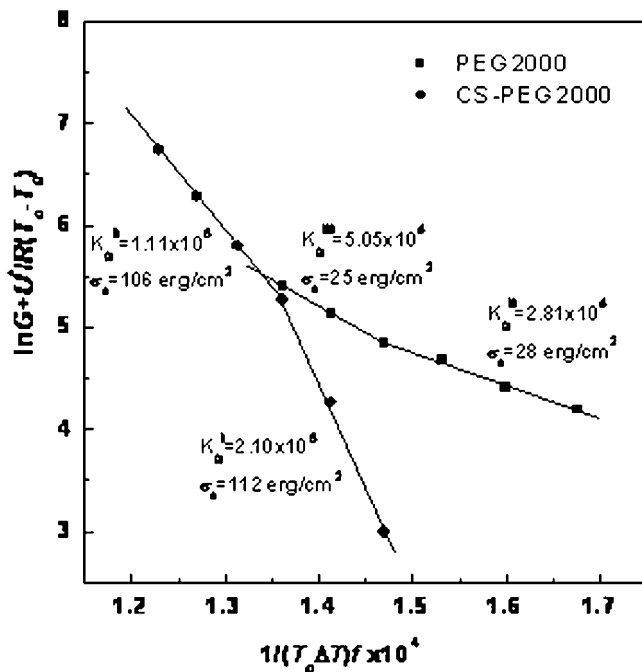


Figure 8 Plots of $\ln G + U^*/R(T_c - T_0)$ versus $1/T_c(\Delta T)f$ for PEG2000 and CS-PEG2000.

deflection in the slope is observed for both samples. It is found that for PEG2000 the slope higher than $T_c = 44^\circ\text{C}$ is nearly half of the slope lower than $T_c = 44^\circ\text{C}$, indicating a transition occurs at $T_c = 44^\circ\text{C}$ from regime III to regime II. In contrast, we notice that in CS-PEG2000 the slope lower than $T_c = 42^\circ\text{C}$ is half of that higher than $T_c = 42^\circ\text{C}$, showing that regimes I and II are observed and the transition is located at $T_c = 42^\circ\text{C}$. This shows that temperature range of crystallization regime is altered by the cholesterol end-group. The free energy of the folding surface (σ_e) can be calculated from the K_g , which is the slope in Figure 8. Assuming that σ is 10 erg/cm^2 , the values of σ_e are 25 and 28 erg/cm^2 for PEG 2000 in regime III and regime II, respectively. These values are very similar to those of PEO homopolymer crystals, 26 erg/cm^2 reported by Kovacs and Cheng.^{23,24} For CS-PEG2000, the values of σ_e are 106 and 112 erg/cm^2 in regime II and regime I, respectively, much higher than those for PEG2000. Therefore, the cholesterol end-group increases the free energy of the folding surface of PEO crystals greatly, which is unfavorable to crystallization of PEG.

SAXS result

The SAXS profiles of PEG2000, CS-PEG2000, and CS-PEG2000-CS are shown in Figure 9. The samples were subject to long time annealing to reach their equilibrium structures. From the positions of SAXS peaks, we can see that lamellar structures are formed

in both samples, since the second SAXS peak appears at $2q^*$ (q^* is the position of the first order SAXS peak.). The long periods (L) can be calculated by $L = 2\pi/q^*$, which are 13.3, 15.4, and 10.7 nm for PEG2000, CS-PEG2000, and CS-PEG2000-CS, respectively. Based on the reported data, the size of extended cholesterol is about 2.0 nm,²⁵ and the length of oxyethylene unit is 0.285 nm when PEG adopts a 7_2 helical conformation in monoclinic crystals.²⁶ As a result, the theoretical long periods can be calculated in terms of folding number of PEG chains and packing of cholesterol. For PEG2000, assuming the PEG chains are extended [Fig. 10(a)], the calculated long period is $L = 0.285 \times 45 = 12.8 \text{ nm}$ (The size of two hydroxyl end groups was not considered.), which agrees well with the long period ($L = 13.1 \text{ nm}$) obtained from SAXS. In CS-PEG2000, if the repeating structure contains single layer of cholesterol and the PEG chains are extended [Fig. 10(b)], the calculated long period for CS-PEG2000 is $L = 2.0 + 0.285 \times 45 = 14.8 \text{ nm}$ (The sizes of methoxyl end group and terephthaloyl coupling reagent were not included). This value is also in accordance with the SAXS result. From SAXS result, we notice that CS-PEG2000-CS has smaller long period than PEG2000 and CS-PEG2000, though this sample contains two bulky cholesterol end-groups. Therefore, we believe that the PEG chains in CS-PEG2000-CS are folded. Assuming the PEG chains are once-folded and the repeating structure included double layers of cholesterol, the calculated long period, which is $L = 2.0 \times 2 + 0.285 \times 45/2 = 10.4 \text{ nm}$ (The size of tereph-

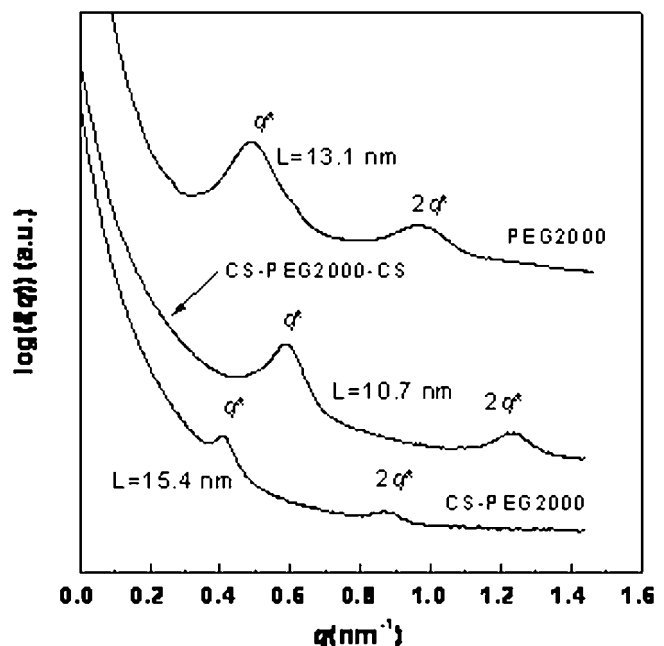


Figure 9 SAXS profiles of PEG2000, CS-PEG2000, and CS-PEG2000-CS after annealing.

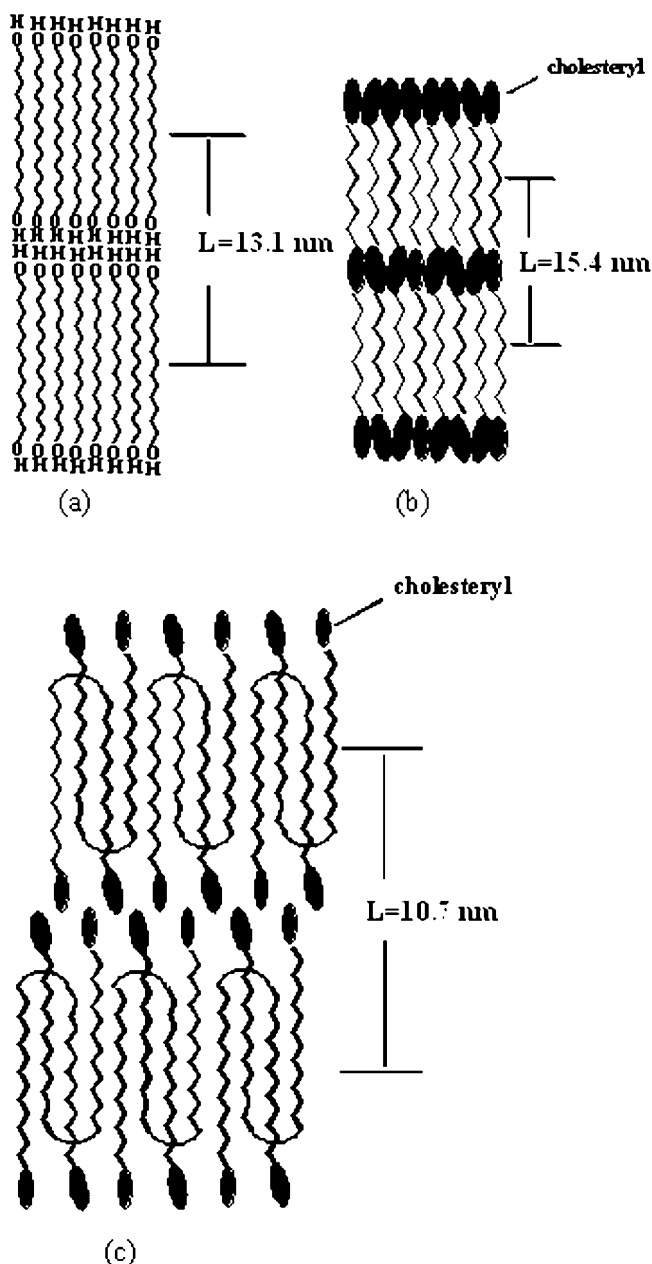


Figure 10 Possible structures of (a) PEG2000, (b) CS-PEG2000, and (c) CS-PEG2000-CS.

thaloyl coupling reagent was not included.), can be comparable to the value from SAXS. As a result, the structure of CS-PEG2000-CS is tentatively like that shown in Figure 10(c). It should be emphasized that we cannot determine the structure of CS-PEG2000-CS from unambiguously. It may also adopt a nonintegral folding conformation. However, we can conclude that the PEG chains are extended in PEG2000 and CS-PEG2000 after long time annealing, but extended conformation can not be reached for CS-PEG2000-CS, even after long time annealing. This is in accordance with the report that large rigid end groups may prevent the transformation of PEG crys-

tals.²⁷ This result can perfectly explain the fact that CS-PEG2000 and PEG2000 have similar melting temperatures, but CS-PEG2000-CS has evidently lower melting temperature, since the melting temperature of polymer crystals is determined by lamellar thickness of crystals.

CONCLUSIONS

The bulky cholesteryl end group can retard crystallization of low molecular weight PEG, especially when both ends of PEG are capped with cholesterol. Isothermal crystallization kinetics shows that the Avrami exponent of CS-PEG2000 abnormally decreases as crystallization temperature. The CS-PEG2000-CS has lower Avrami exponent. Perfect spherulites are observed in PEG2000, and CS-PEG2000 exhibits irregular leaf-like spherulites morphology, while only needle-like crystals, instead of spherulites, are observed in CS-PEG2000-CS. Crystallization temperature has a greater influence on linear growth rate of CS-PEG2000 than PEG2000. The cholesterol end-group can change both the free energy of the folding surface and the temperature range of crystallization regime. The SAXS results show that the PEG chains are extended in PEG2000 and CS-PEG2000, but they are once-folded in CS-PEG2000-CS.

References

- Borman, C. D.; Jackson, A. T.; Bunn, A.; Cutter, A. L.; Irvine, D. J. *Polymer* 2000, 41, 6015.
- Lee, S. H.; Kim, S. H.; Han, Y. K.; Kim, Y. H. *J Polym Sci, Part A: Polym Chem* 2001, 39, 973.
- Ogawa, R.; Nagasaki, Y.; Murata, T. *Kobunshi Ronbunshu* 2002, 59, 702.
- Hu, Y. H.; Chen, C. Y. *Polym Degrad Stab* 2003, 80, 1.
- Kenwright, A. M.; Peace, S. K.; Richards, R. W.; Bunn, A.; MacDonald, W. A. *Polymer* 1999, 40, 5851.
- Kenwright, A. M.; Peace, S. K.; Richards, R. W.; Bunn, A.; MacDonald, W. A. *Polymer* 1999, 40, 2035.
- Huang, Z. H.; Chen, S.; Huang, J. L. *J Appl Polym Sci* 1999, 73, 1379.
- Dormidontova, E. E. *Macromolecules* 2004, 37, 7747.
- Li, L. J.; Yang, M. H. *Polymer* 1998, 39, 689.
- Cheng, S. Z. D.; Chen, J. H.; Heberer, D. P. *Polymer* 1992, 33, 1429.
- Cheng, S. Z. D.; Wu, S. S.; Chen, J. H.; Zhou, Q. Z.; Quirk, R. P.; von Meerwall, E. D.; Hsiao, B. S.; Habenschuss, A.; Zschack, P. R. *Macromolecules* 1993, 26, 5105.
- Shibaev, L. A.; Antonova, T. A.; Vinogradova, L. V.; Ginzburg, B. M.; Zgonnik, V. N.; Melenevskaya, E. Y. *Tech Phys Lett* 1997, 23, 704.
- Zgonnik, V. N.; Vinogradova, L. V.; Melenevskaya, E. Y.; Litvinova, L. S.; Kever, E. E.; Bykova, E. N.; Klenin, S. I. *Russ J Appl Chem* 1997, 70, 1098.
- Ginzburg, B. M.; Goloudina, S. I.; Vinogradova, L. V.; Zgonnik, V. N.; Melenevskaya, E. Y. *Tech Phys Lett* 1998, 24, 495.
- Yao, N.; Jamieson, A. M. *Polymer* 2000, 41, 2925.

16. Dong, B. Z.; Sheng, W. J.; Yang, H. L.; Zhang, Z. J. *J Appl Crystallogr* 1997, 30, 877.
17. Lopez-Quintela, M. A.; Akahane, A.; Rodriguez, C.; Kunieda, H. *J Colloid Interface Sci* 2002, 247, 186.
18. Godovsky, Y. K.; Slonimsky, G. L.; Garbar, N. M. *J Polym Sci C* 1972, 38, 1.
19. Cheng, S. Z. D.; Wunderlich, B. *J Polym Sci, Part B: Polym Phys* 1986, 24, 595.
20. Xu, J. T.; Fairclough, J. P. A.; Mai, S. M.; Ryan, A. J.; Chaibundit, C. *Macromolecules* 2002, 35, 6937.
21. Lauritzen, J. I.; Hoffman, J. D. *J Appl Phys* 1973, 44, 4340.
22. Mark, J. E. *Polymer Data Handbook*; Oxford: Oxford University Press, 1999.
23. Kovacs, A. J.; Gonithier, A. *Kolloid Z Z Polym* 1972, 250, 530.
24. Cheng, S. Z. D.; Chen, J. H.; Janimak, J. J. *Polymer* 1990, 31, 1018.
25. Loomis, C.; Shipley, G.; Small, D. *J Lipid Res* 1979, 20, 525.
26. Craven, J. R.; Zhang, H.; Booth, C. *J Chem Soc Faraday Trans* 1991, 87, 1183.
27. Huang, Y.; Wang, J.; Liu, X. B.; Zhang, H. L.; Chen, X. F.; Zhuang, W. C.; Chen, X.; Ye, C.; Wan, X. H.; Chen, E. Q.; Zhou, Q. *F. Polymer* 2005, 46, 10148.